



A polyolefin encapsulant material designed for photovoltaic modules: from perspectives of peel strength and transmittance

Bo Lin^{1,3} · Chen Zheng² · Qingying Zhu¹ · Fang Xie¹

Received: 27 April 2019 / Accepted: 1 November 2019 / Published online: 11 November 2019
© Akadémiai Kiadó, Budapest, Hungary 2019

Abstract

A secondary master batch process had been applied to design a polyolefin encapsulant material for photovoltaic modules, in which the polymer blend was composed of polyolefin elastomer (POE) and linear low-density polyethylene (LLDPE) with the addition of the cross-linking agent of *tert*-butylperoxy 2-ethylhexyl carbonate (TBEC) and silane coupling agent of γ -methacryloxypropyl trimethoxy silane (KH570). The rheological property from Haake torque rheometer illuminated that the chemical cross-linking reaction could take place between the POE and TBEC. The LLDPE was added for further increasing the cohesion of polymer blend by obtaining much more physical cross-linking points from the physical entanglement between the flexible chains of LLDPE and the amorphous zone of POE. However, the transmittance of polymer blend ran down with the rise of LLDPE content within the polymer blend. The number and site of melting points of polymer blend by the DSC analysis show that there was compatibility between the POE and LLDPE within the polymer blend; meanwhile, the resultant molecular structures of the polymer blend also had been explained by the FTIR spectra. These results unanimously illuminated that it was a feasible solution for fabricating the polyolefin encapsulant material for photovoltaic modules.

Keywords Polyolefin elastomer · Polymer blend · Rheological property · Transmittance · Peel strength

Introduction

Long durability of photovoltaic (PV) modules was critical to reduce the lifespan cost in the solar cells [1–4]. However, the ability to maintain the stability of PV module efficiency under long-term and harsh environment conditions mostly relied on reliable encapsulant materials that they should have the characteristics of high transmittance, strong adhesion between the encapsulant and substrate, low interface conductivity, and low moisture permeation [1].

Synthetic polymers have been playing an increasingly important role as the encapsulation materials in PV modules in recent years [5, 6]. Ethylene–vinyl acetate (EVA) was a copolymer of ethylene and vinyl acetate, and it was a thermoplastic elastomer (without vulcanization) with high flexibility and toughness, widely used in the plastic industry, especially, commonly used as encapsulant material for crystalline silicon solar cells [7, 8]; however, it was not conducive to the repairing of defective PV modules, which was due to the EVA film was not prominent enough in its aging resistance and the chemical reaction of cross-linking during the processing. Therefore, there were some new encapsulant materials in the field of industry which can replace the EVA, such as thermoplastic urethanes, polyolefin encapsulant materials, polyvinyl butyral, and thermoplastic silicone elastomer [9–12]. Among them, the polyolefin encapsulant materials had their great market prospects because of their low price and high encapsulant efficiency.

Polyolefin elastomer (POE) was a copolymer of ethylene and octylene whose crystallization property was mainly affected by the content and spatial distribution of octyl in the POE [13, 14]. Although the aging resistance of POE was excellent, its cohesion was small for the POE was a saturated

✉ Bo Lin
jidalinbo@163.com

✉ Chen Zheng
zhengchenkenaf@163.com

¹ School of Chemistry and Materials Engineering, Huizhou University, Huizhou 516007, Guangdong, China

² Glorious Sun Guangdong School of Fashion, Huizhou University, Huizhou 516007, Guangdong, China

³ Guangzhou Lushan New Materials Co., Ltd, No 22, Pubei Road, Yunpu Industrial Zone, Huangpu, Guangzhou 510530, China

polyolefin material. What is more, the POE can exhibit high transmittance, persistent bonding, and good creep resistance with the small deformation [1, 3, 4, 15–18]. It was considered to be designed as one of the polymeric encapsulants for the photovoltaic modules in solar cell, which can adapt to harsh environment such as the high and low temperature cycle [5, 6, 10, 15].

This work focused on developing a suitable and new PV encapsulation material instead of EVA that was commonly used for the crystalline silicon solar cell. For this purpose, the LLDPE had been added into the pristine POE to obtain much more physical cross-linking points for improving its cohesion and creep resistance, and then the expected polymer blend POE/LLDPE with the additives of *tert*-butylperoxy 2-ethylhexyl carbonate (TBEC) and γ -methacryloxypropyl trimethoxy silane (KH570) had been granulated evenly with a secondary master batch process, and finally the optical performance analysis and the peel strength measurement could confirm that it was feasible for the design solution on the polyolefin encapsulant material for PV modules in crystalline silicon solar cells.

Experimental

Materials

Polyolefin elastomer (POE) was bought from Dow Chemical Company, linear low-density polyethylene (LLDPE) was obtained from SINOPEC Maoming Petrochemical Branch, *tert*-butylperoxy 2-ethylhexyl carbonate (TBEC, 99.5 mass%) was purchased from Tokyo Chemical Industry, γ -methacryloxypropyl trimethoxy silane (KH570, ≥ 97.0 mass%) was provided from Shanghai Reagents Company. The borosilicate glass plates of 3.2 mm thickness, the ribbons of 2 mm width, and the backsheet used for adhesion measurement were supplied by Guangzhou Chemical Reagent Factory.

Sample preparation

The polymer compounds of POE/TBEC (POE/TBEC was the abbreviation of the compound between POE and TBEC), POE/TBEC/KH570, POE/LLDPE/TBEC, and POE/LLDPE/TBEC/KH570 with the appointed formula (Tables 1 and 4) had been mixed well by a mechanical stirrer (SHR-10A, Laizhou Jintai Chemical Industry, China), and then each polymer compound was granulated by a plastic extruder (SJZS-10B-SZS-20,

Ruiming Plastic Machinery Manufacturing Plant, China) at 140 °C.

Measurements

The laminator curing adopted in this work by using an automatic laminating machine for solar photovoltaic modules (KSL2345OAC-C/D, QHD Visual Automation Equipment Co., Ltd.). The sample of lamination process was loaded at 50 °C with 200 Pa, heated to 85 °C for 6 min, and heated to 110 °C for 2 min, and pressure was then applied to a diaphragm on top of the samples. After that, the sample was heated to 150 °C for 8 min, cooled down to 85 °C, and finally vented to atmospheric pressure. The samples for optical performance test with a lamellae structure of glass slide/polymeric film/glass slide were compounded in the laminator. The curing of sample for the peel strength measurement was operated on a press vulcanizer (BFC-25T, Panstone, China) with a clamping force of 25 MN and a plate unit pressure of 14 MPa. The curing process by the press vulcanizer was carried out at 140 °C and lasted for 40 min. The peel strength measurement of the samples was carried out using an American standard test method (ASTM) D903-98 with a separation angle of approximately 180 ° and a separation rate of 152 mm min⁻¹ at the room temperature of 25 °C [1]. The sample for peel measurement adopted a compound mode of polymer blend/PET backsheet. The cross-linking degree measurement of the samples was dealt with GB/T 36965-2018 of China that the test method for cross-linking degree of ethylene–vinyl acetate copolymer applied in photovoltaic modules—differential scanning calorimetry (DSC). The data of rheological property were adopted by Haake torque rheometer (Haake Rheocord 9000, German). The ultraviolet–visible light transmission analysis of samples was conducted by a HITACHI U-3010 spectrophotometer with a compound mode of glass/polymer blend/glass. The melting points of the polymer and the polymer blend were measured by differential scanning calorimeter (DSC, Netzsch DSC 200-PC) and operated in N₂ atmosphere. The DSC instrument was calibrated with an indium standard, and Al was used as reference material. Each sample of about 10 mg was scanned at a heating rate of 10 °C min⁻¹. The Fourier transform infrared spectroscopy (FTIR) spectra were obtained on a Magna-550 FTIR instrument for analyzing the molecular structure of the POE and the polymer blend. The sample films were directly prepared from the POE or the polymer blend by the press vulcanizer and used for FTIR analysis.

Table 1 Composition of the chemical cross-linking system POE/TBEC/KH570 based on weight parts (phr, per hundred of resin)

Entry	POE	TBEC	KH570
1	100	1.5	–
2	100	1.5	0.3
3	100	1.5	0.7

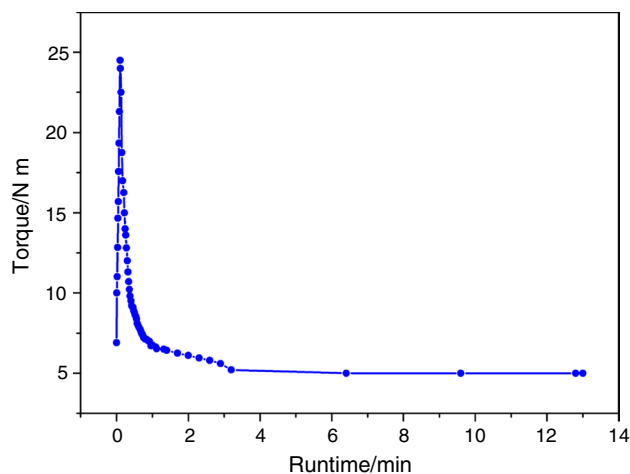


Fig. 1 Rheological property of the pristine POE

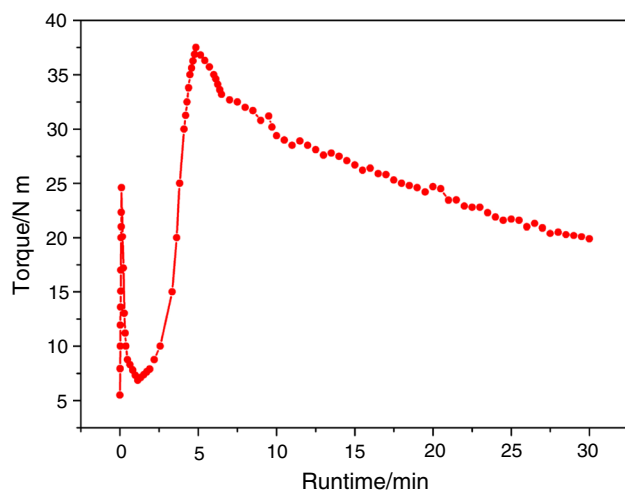


Fig. 2 Rheological property of the chemical cross-linking system with a mass ratio of $m_{\text{POE}}/m_{\text{TBEC}} = 100:1.5$

Results and discussion

The chemical cross-linking of POE without LLDPE

The rheological data of the pristine POE and the polymer compound POE/TBEC had been obtained by Haake torque rheometer with a rotational speed of 50 r min^{-1} at $150 \text{ }^\circ\text{C}$ as shown in Figs. 1 and 2, respectively. Contrasting with the rheological data of the pristine POE (Fig. 1), Fig. 2 shows that a cross-linking reaction occurred after the addition of the peroxide initiator (namely the cross-linking agent) of TBEC into the pristine POE at the run time of 1.1 min, the molecular chain of the POE changed from linear structure to three-dimensional network structure, and the viscosity of the polymer compound increased at the

Table 2 Cross-linking degree of the chemical cross-linking system shown in Table 1 with two different curing processes

Entry	Laminator curing/mass%	Curing of press vulcanizer/mass%
1	5.2	76.0
2	6.5	84.2
3	12.8	89.4

Table 3 Peel strength of the chemical cross-linking system shown in Table 1 with two different curing processes

Entry	Laminator curing/ N cm^{-1}	Curing of press vulcanizer/ N cm^{-1}
1	12	48
2	15	56
3	18	72

same time, and it presented an obvious rise of the torque with increasing the run time from 1.1 to 4.8 min. Therefore, the rise of the torque curve can be used as a marker of the beginning of the cross-linking reaction. Moreover, the slope of the rising curve for the torque reflected that there was a faster speed of cross-linking reaction for the polymer compound POE/TBEC that had taken place as well. However, these could not be observed in the case of pristine POE (Fig. 1).

To clarify the role of the silane coupling agent of KH570, the results of cross-linking degree for the polymer compound with different mass parts of KH570 (Table 1) show that it was less than 12.8 mass% for the laminator curing (Table 2). It meant that it was difficult to take place the obvious cross-linking reaction throughout the polymer compound within a relatively short period of curing time (16 min). However, the polymer compound could obtain a much bigger cross-linking degree (76.0–89.4 mass%) resulting from the curing process which was operated on the press vulcanizer with a long time for 40 min. It concluded that the chemical cross-linking reaction took place in a difficult manner and need much more energy consumption for the single polymer component of POE. The grafting of KH570 would be more practicable to solve this shortcoming for the cross-linking degree increasing with the mass parts of KH570 (Table 2). Table 3 shows that the adhesion of samples with a certain amount of KH570 was more than that from the sample without KH570 for different curing processes of laminator curing and press vulcanizer. Since the POE used in this work had less adhesion, the silane coupling agent of KH570 had been added into the POE with an obvious promotion for the adhesion of samples as shown in Table 3. Therefore, the above results consistently proved that the grafting of KH570 onto the POE

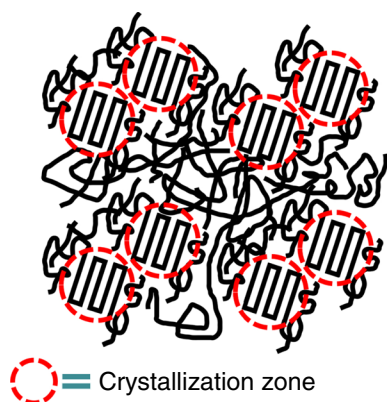


Fig. 3 A scheme of physical entanglement between the LLDPE and POE within the polymer blend POE/LLDPE. The red dotted circle represented the crystallization zone of the POE, while the flexible chains (black line) from LLDPE and POE were interlaced together in the amorphous zone. (Color figure online)

can both improve the cross-linking degree and the adhesion of POE.

The chemical cross-linking of POE with LLDPE

In order to improve further the cohesion of POE, one of the most effective methods was the addition of LLDPE into POE to obtain much more physical cross-linking points from the physical entanglement between the flexible chains of LLDPE and the amorphous zone of POE as shown in Fig. 3. Based on this reason, the POE and the LLDPE had been mixed as full as possible before the cross-linking reactions took place. The resultant peel strength of polymer blends is shown in Fig. 4. It was shown that the peel strength of polymer blends changed with the content of LLDPE in the polymer blend with a mass ratio of $m_{\text{POE}}/m_{\text{LLDPE}}/m_{\text{TBEC}} = 100:n:1.5$, in which the n represented the mass parts of LLDPE that was added into POE for each appointed formula of polymer blends. It displayed that the cohesion of polymer blends was more than 60 N cm^{-1} that was the standard cohesion of EVA used commonly as encapsulant in the solar cell when the content of LLDPE in the polymer blend was $n \geq 4$.

Table 4 Composition of the chemical cross-linking system POE/LLDPE/TBEC/KH570 based on weight parts (phr, per hundred of resin)

Sample 1/phr	Sample 2/phr	Sample 3/phr
POE: 75	Sample 1: 20	POE: 95
LLDPE: 25	POE: 80	LLDPE: 5
TBEC: 7.5		TBEC: 1.5
KH570: 3		KH570: 0.6

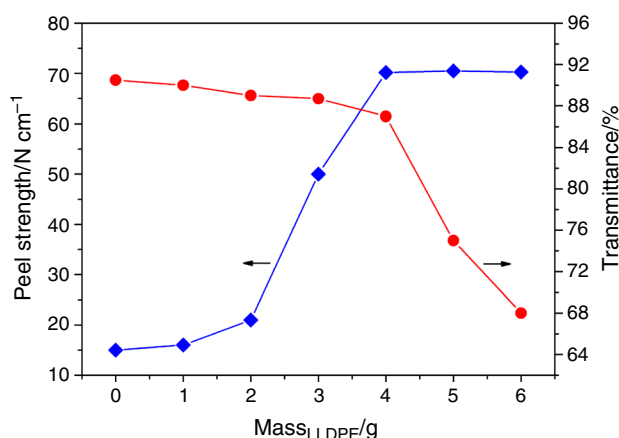


Fig. 4 Peel strength and transmittance of the polymer blends with a mass ratio of $m_{\text{POE}}/m_{\text{LLDPE}}/m_{\text{TBEC}} = 100:n:1.5$, where n represented the weight parts of LLDPE in the polymer blends. The transmittance of polymer blend was adopted at a wavelength of 520 nm

Nevertheless, when the content of LLDPE increased to $n = 5$, the cohesion of polymer blends could not be absolutely controlled by the increment of the physical cross-linking point. Figure 4 also shows that the cohesion of pristine POE ($n = 0$) was less than that of the polymer blends with LLDPE ($n > 0$), for the grafting amount of the cross-linking agent (TBEC) onto the pristine POE was less than that of POE/LLDPE blends. It meant that the TBEC used here was more active to the external LLDPE in contrast with the single component of POE. In other words, the LLDPE could directly improve the adhesion of polymer blends. Consequently, the addition of LLDPE could help us to improve the creep resistance of POE, especially used for encapsulant, and plays an important role in the dimensional stability under different conditions of external environment temperature.

On the other hand, the silane coupling agent (KH570) had been also added into the polymer blend POE/LLDPE/TBEC (Table 4) to define the formula of the polyolefin encapsulant material designed for photovoltaic modules. The DSC curves of the POE and the chemical cross-linking system compounded by POE and LLDPE are presented in Fig. 5. The thermal behavior of the POE and its corresponding polymer blend both show that there were almost two identical melting points. They were $44 \text{ }^\circ\text{C}$ and $66 \text{ }^\circ\text{C}$ for the POE (Fig. 5a), and melting points were $45 \text{ }^\circ\text{C}$ and $64 \text{ }^\circ\text{C}$ for the polymer blend (Fig. 5b). Multiple melt peaks in the POE and its polymer blend were ascribed to different crystalline polymorphs that were also present in their common composition of polyolefin. However, it was quite different for the latter on the melt behavior, and the polymer blend displayed a quite higher melting point located at $114 \text{ }^\circ\text{C}$, because the LLDPE had been artificially added into the polymer blend. Therefore, it made the melting point shift toward the higher temperature range than that of the POE. It was noted that

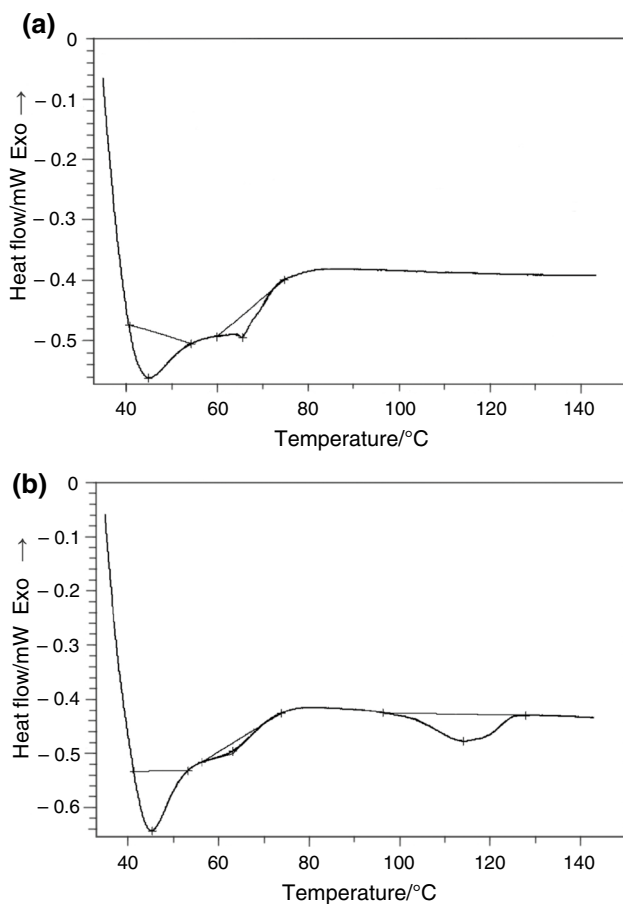


Fig. 5 DSC curves of the pristine POE (a) and the polymer blend POE/LLDPE/TBEC/KH570 (b). The polymer blend was adopted from sample 2 in Table 4

the number of the third melting point of polymer blend was smaller than that of the pristine LLDPE of 120 °C, which illuminated that there was certain compatibility between the POE and LLDPE within the polymer blend. Consequently, it made the melting pointing move to the lower range of temperature than that of the pristine LLDPE as shown in Fig. 5b. These data confirmed that the chemical cross-linking reaction had taken place in the polymer blend POE/LLDPE/TBEC/KH570.

The FTIR spectra of the POE and the polymer blend POE/LLDPE/TBEC/KH570 had been obtained and are shown in Fig. 6. In the FTIR spectra, the peak sites of 2920–2940 cm^{-1} and 2850–2870 cm^{-1} were corresponding to the asymmetric stretching vibration and symmetric stretching vibration of methylene, respectively. Meanwhile, the absorption peak located at 1465 cm^{-1} was ascribed to the bending vibrations of methylene from POE and polymer blend, and 720 cm^{-1} was the peak site for rocking vibration from the group of $-(\text{CH}_2)_n-$ ($n \geq 4$). These data show that the FTIR spectrum of the POE (Fig. 6a) and polymer blend (Fig. 6b) was very similar; however, the

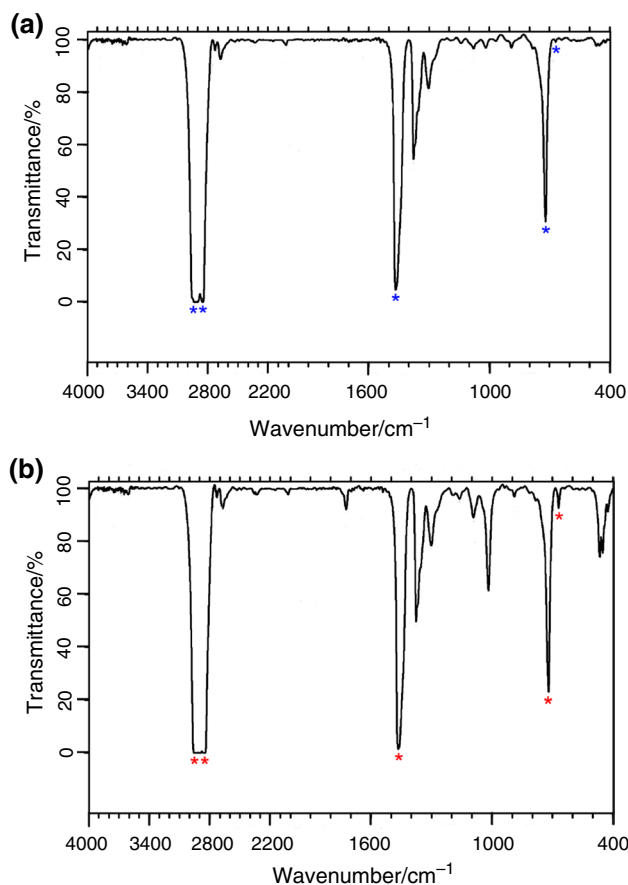


Fig. 6 FTIR spectra of the pristine POE (a) and the polymer blend POE/LLDPE/TBEC/KH570 (b). The polymer blend was adopted from sample 2 in Table 4

dual crystalline peaks between 720 and 670 cm^{-1} appeared in the polymer blend, which illuminated a crystalline polymer of LLDPE lay in the polymer blend (Fig. 6b). On the other hand, the absorption peak intensity that is located at 1018 cm^{-1} of the polymer blend (Fig. 6b) was stronger than that of the pristine POE (Fig. 6a), which confirmed that the content of methyl in the polymer blend was higher than that of the POE, for the branching degree of polymer chain of the LLDPE was higher than that of the POE. The data from FTIR confirmed again that the cross-linking reaction had been taken place in the polymer blend POE/LLDPE/TBEC/KH570.

Figure 7 shows the transmittance of the pristine POE and the polymer blend POE/LLDPE/TBEC/KH570. The transmittance of polymer blend (sample 2 in Table 4) increased rapidly between 310 nm and 550 nm and reached a maximum number in the transmittance of 86.4% at 550 nm and then decreased slowly after 550 nm. The transmittance of pristine POE was higher than that of the polymer blend between 310 and 550 nm. These data show that the addition of the opaque LLDPE made the transmittance of the

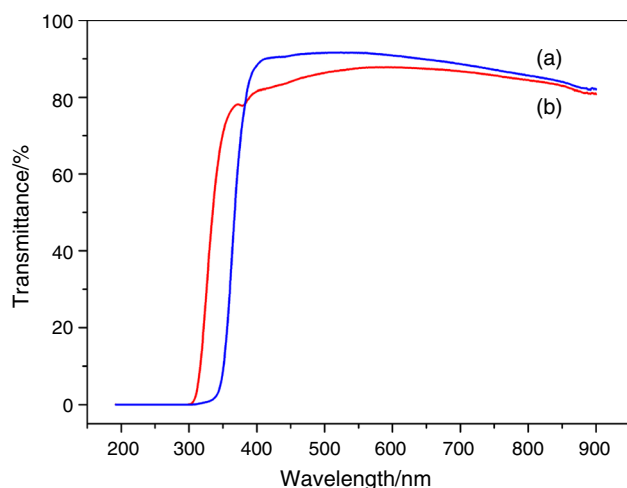


Fig. 7 Ultraviolet–visible light transmittance of the pristine POE (a) and the polymer blend POE/LLDPE/TBEC/KH570 (b). The polymer blend was adopted from sample 2 in Table 4

Table 5 Optical performance and peel strength for the chemical cross-linking system POE/LLDPE/TBEC/KH570 with the formula adopted from Table 4

Performance	Sample 2	Sample 3	POE
UV–Vis transmittance/%	86.4	79.7	88.0
Haze/%	6.2	14.4	3.1
Peel strength/ N cm^{-1}	65.2	59.5	12.0

polymer blend lower than that of the pristine POE. Table 5 shows that the transmittance of sample 3 was less than that of the sample 2, even though they both had same mass parts of 5 phr LLDPE in the polymer blends, for a secondary master batch process method had been adopted by sample 2 to get the chemical cross-linking system. Contrasting with the pristine POE, the transmittance of sample 2 and sample 3 were less than that of the pristine POE as shown in Table 5. It illuminated that the transmittance might be affected most by the polymers from the cross-linking system. From Table 5, it also deduced that the transmittance measured by UV–Vis spectrophotometer had more relevance on the characterization of the transparency for the polymer blends. The transmittance of sample 2 was higher than that of sample 3; meanwhile, the haze of the former (6.2%) was superior to latter (14.4%), which kept consistent in their optical performance. It was due to a secondary master batch process had been adopted by sample 2, which made the polymers and additives mixing more evenly. It also meant that if the mass parts of LLDPE in the cross-linking material system were further reduced and the LLDPE was uniformly dispersed, then the effect of LLDPE on optical properties should be smaller, which could be confirmed by the relationship

between the transmittance and the mass parts of LLDPE in the chemical cross-linking system as shown in Fig. 3.

Conclusions

In this work, a polyolefin encapsulant material designed for photovoltaic modules had been successfully prepared with a secondary master batch process by compounding polyolefin elastomer (POE) and linear low-density polyethylene (LLDPE) with the addition of the small molecular additives of the cross-linking agent of *tert*-butylperoxy 2-ethylhexyl carbonate (TBEC) and the silane coupling agent of γ -methacryloxypropyl trimethoxy silane (KH570). Haake torque rheometer shows that there was an obvious rise of the torque with run time ranging from 1.1 to 4.8 min, which illuminated that the chemical cross-linking process between the POE and TBEC was feasible. The KH570 and LLDPE had been added in sequence to increase the cross-linking degree and the cohesion for the polymer blend. The compatibility between the POE and LLDPE had been proved from the data of melting point peaks by DSC analysis. The dual peaks between 720 and 670 cm^{-1} were taken as another proof for the existence of LLDPE from FTIR. It was concluded that the polymer blend with a mass ratio of $m\text{POE}/m\text{LLDPE}/m\text{TBEC}/m\text{KH570}=95:5:1.5:0.6$ and taking the transmittance of 86.4% and the peel strength of 65.2 N cm^{-1} , which used as encapsulant material was feasible for the photovoltaic modules.

Acknowledgements B.L. gratefully acknowledged for financial supports from the professorial and doctoral scientific research foundation of Huizhou University (Grant No. 2018JB001) and the Science Foundation of Guangdong Province (Grant No. 2017A030313080).

References

- Hsu HY, Hsieh HH, Tuan HY, Hwang JL. Oxidized low density polyethylene: a potential cost-effective, stable, and recyclable polymeric encapsulant for photovoltaic modules. *Sol Energy Mater Sol Cells*. 2010;94:955–9. <https://doi.org/10.1016/j.solmat.2010.01.020>.
- Zweibel K. Thin film PV manufacturing: materials costs and their optimization. *Sol Energy Mater Sol Cells*. 2000;63:375–86. [https://doi.org/10.1016/S0927-0248\(00\)00057-X](https://doi.org/10.1016/S0927-0248(00)00057-X).
- Pan K, Zeng X, Li H, Lai X, Huang J. Synthesis of an adhesion-enhancing polyhydrosiloxane containing acrylate groups and its cross-linked addition-cure silicone encapsulant. *J Elastom Plast*. 2013;47:416–30. <https://doi.org/10.1177/0095244313514992>.
- Pan K, Zeng X, Li H, Lai X. Synthesis of siloxanes containing vinyl and epoxy group and its enhancement for adhesion of addition-cure silicone encapsulant. *J Macromol Sci A*. 2013;50:1126–32. <https://doi.org/10.1080/10601325.2013.829361>.
- Hintersteiner I, Sternbauer L, Beissmann S, Buchberger WW, Wallner GM. Determination of stabilisers in polymeric

- materials used as encapsulants in photovoltaic modules. *Polym Test*. 2014;33:172–8. <https://doi.org/10.1016/j.polymertesting.2013.12.004>.
6. Snaith HJ, Hacked P. Enabling reliability assessments of pre-commercial perovskite photovoltaics with lessons learned from industrial standards. *Nat Energy*. 2018;3:459–65. <https://doi.org/10.1038/s41560-018-0174-4>.
 7. Tábi T. The application of the synergistic effect between the crystal structure of poly(lactic acid) (PLA) and the presence of ethylene vinyl acetate copolymer (EVA) to produce highly ductile PLA/EVA blends. *J Therm Anal Calorim*. 2019. <https://doi.org/10.1007/s10973-019-08184-x>.
 8. Yang G, Wu W, Dong H, Wang Y, Qu H, Xu J. Synergistic flame-retardant effects of aluminum phosphate and Trimer in ethylene-vinyl acetate composites. *J Therm Anal Calorim*. 2018;132:919–26. <https://doi.org/10.1007/s10973-018-7026-0>.
 9. Peike C, Hülsmann P, Blüml M, Schmid P, Weiß KA, Köhl M. Impact of permeation properties and backsheets-encapsulant interactions on the reliability of PV modules. *ISRN Renew Energy*. 2012. <https://doi.org/10.5402/2012/459731>.
 10. Luo W, Khoo YS, Hacked P, Naumann V, Lausch D, Harvey SP, Singh JP, Chai J, Wang Y, Aberle AG, Ramakrishna S. Potential-induced degradation in photovoltaic modules: a critical review. *Energy Environ Sci*. 2017;10:43–68. <https://doi.org/10.1039/C6EE02271E>.
 11. Ferrada P, Marzo A, Cabrera E, Chu H, Campo V, Rabanal J, Diaz-Almeida D, Schneider A, Kopecek R. Potential for photogenerated current for silicon based photovoltaic modules in the Atacama Desert. *Sol Energy*. 2017;144:580–93. <https://doi.org/10.1016/j.solener.2017.01.053>.
 12. Ottersböck B, Oreski G, Pinter G. Comparison of different microclimate effects on the aging behavior of encapsulation materials used in photovoltaic modules. *Polym Degrad Stabil*. 2017;138:182–91. <https://doi.org/10.1016/j.polymdegradstab.2017.03.010>.
 13. Mochane MJ, Mokhena TC, Motaung TE, Linganis LZ. Shape-stabilized phase change materials of polyolefin/wax blends and their composites. *J Therm Anal Calorim*. 2019. <https://doi.org/10.1007/s10973-019-08734-3>.
 14. Wen X, Szymańska K, Chen X, Mijowska E. Nanosized carbon black as synergist in PP/POE-MA/IFR system for simultaneously improving thermal, electrical and mechanical properties. *J Therm Anal Calorim*. 2019. <https://doi.org/10.1007/s10973-019-08466-4>.
 15. López-Escalante MC, Caballero LJ, Martín Gabás FM, Cuevas A, Ramos-Barrado JR. Polyolefin as PID-resistant encapsulant material in PV modules. *Sol Energy Mater Sol Cells*. 2016;144:691–9. <https://doi.org/10.1016/j.solmat.2015.10.009>.
 16. Oliveira MCC, Cardoso ASAD, Viana MM, Freitas Cunha Lins V. The causes and effects of degradation of encapsulant ethylene vinyl acetate copolymer (EVA) in crystalline silicon photovoltaic modules: a review. *Renew Sustain Energy Rev*. 2018;81:2299–317. <https://doi.org/10.1016/j.rser.2017.06.039>.
 17. López-Escalante MC, Fernández-Rodríguez M, Caballero LJ, Martín F, Gabás M, Ramos-Barrado JR. Novel encapsulant architecture on the road to photovoltaic module power output increase. *Appl Energy*. 2018;228:1901–10. <https://doi.org/10.1016/j.apenergy.2018.07.073>.
 18. Omazic A, Oreski G, Halwachs M, Eder GC, Hirschl C, Neumaier CL, Pinter G, Erceg M. Relation between degradation of polymeric components in crystalline silicon PV module and climatic conditions: a literature review. *Sol Energy Mater Sol Cells*. 2019;192:123–33. <https://doi.org/10.1016/j.solmat.2018.12.027>.

Publisher's Note Springer Nature remains neutral with regard to jurisdictional claims in published maps and institutional affiliations.